3D-QSAR CoMFA and CoMSIA studies on a set of diverse alpha(1a)-adrenergic receptor antagonists

ARTICLE *in* MEDICINAL CHEMISTRY RESEARCH · DECEMBER 2011

Impact Factor: 1.4 · DOI: 10.1007/s00044-010-9379-1

2 AUTHORS:

Amit K Gupta
University of Texas Health Science Center at …
14 PUBLICATIONS **69** CITATIONS
SEE PROFILE

Anil Kumar Saxena
Central Drug Research Institute
166 PUBLICATIONS **1,326** CITATIONS
SEE PROFILE

MEDICINAL CHEMISTRY RESEARCH2011, 20 (9), 1455-1464

3D-QSAR CoMFA AND CoMSIA STUDIES ON A SET OF DIVERSE α_{1a}-ADRENERGIC RECEPTOR ANTAGONISTS†

Amit K. Gupta · Anil K. Saxena*

*Medicinal and Process Chemistry Division, Central Drug Research Institute, C.S.I.R., Lucknow, 226001, India. Tel: +9152226124112/ex 4386, Fax: +9152226123405. E-mail: anilsak@gmail.com

Abstract

The α-adrenergic receptors (α-ARs) modulate a number of intracellular processes and among these α_{1a}- adrenergic receptors play an important role in the regulation of physiological processes related to cardiovascular system. In view of its therapeutic potential, comparative molecular field analysis (CoMFA) and comparative molecular similarity indices analysis (CoMSIA) studies were performed on a diverse set of α-adrenergic receptor antagonists to understand the structural factors affecting their antagonist activity. Both CoMFA (q^2 = 0.709, r^2 = 0.962, and $r^2_{\text{predictive}}$ = 0.629) and CoMSIA (q^2 = 0.648, r^2 = 0.949, and $r^2_{\text{predictive}}$ = 0.656) models gave statistical significant results. The generated CoMFA & CoMSIA models suggest that steric, electrostatic and hydrophobic interactions play an important role in describing the variation in antagonistic activity. The models may be useful in the identification and optimization of novel scaffolds with potent α_{1a} –adrenergic receptor antagonistic activity.

Keywords: Adrenergic receptors · 3D-QSAR · CoMFA · CoMSIA · Drug Design

Introduction

The Human adrenergic receptors are member of G-protein coupled receptors (GPCRs) family and all contains seven anti-parallel transmembrane helices. There are nine different adrenergic receptors which fall into three different classes: α_1, α_2 and β, each class consisting of three subtypes of receptors. The α-adrenergic receptors (α-ARs) play a pivotal role in the regulation of a variety of physiological processes, particularly within the cardiovascular system and are divided into two main subtypes namely α_1- and α_2-ARs (Kulig *et al.*, 2009). The α_1-adrenergic receptors are widely distributed throughout the body and mediate number of physiological functions. The α_1-ARs are mainly present in blood vessels (postsynaptic), smooth muscle (postsynaptic), heart (postsynaptic), eyes (postsynaptic), liver (postsynaptic), CNS (postsynaptic), sympathetic neurons (presynaptic) (Jain *et al.*, 2008). In addition to blood pressure reduction, α_1-ARs antagonists also show beneficiary effect on plasma lipoproteins. Recent study revealed that activation of α_{1a}-ARs may be responsible for ischemia-induced cardiac arrhythmia. Therefore α_{1A}-ARs antagonists could be useful for the treatment of ischemia-induced cardiac arrhythmia (MacDougall *et al.*, 2006).

The binding site analysis of full-length α_{1a}-AR using homology modeling and molecular docking has been carried out (Pedretti *et al.*, 2004; Evers et al., 2005). There are relatively few publications reporting the application of QSAR analysis to α_1-ARs species (Debnath *et al.*, 2003; Fumagalli *et al.*, 2005; Pallavicini *et al.* 2006; Shakya *et al.*, 2006; Nowaczyk *et al.*, 2009). The general α_1-ARs pharmacophore developed by Barbaro *et al.* was based on pyridazinone derivatives(Barbaro *et al.*, 2001; Fang *et al.*, 2003) while Li *et al.* developed an α_{1a} pharmacophore based on a diverse class of compounds(Li *et al.*, 2005). Recently, selective

pharmacophore for α_1-ARs subtype was developed by MacDougall *et al.* (MacDougall *et al.*, 2006). A CoMFA study on hexahydro and octahydropyrido[1,2-c]pyrimidine derivatives as α_{1a}-AR antagonists has been reported (Maciejewska *et al.*, 2006) while a Self-Organizing Molecular Field Analysis (SOMFA) method to provide insight for the development of α_1-adrenoceptor antagonists has been carried out by Li *et al.*(Li *et al.*, 2007).

Since the exact crystal structure of α_{1a}-adrenoreceptor is unknown and a little attention has been given to the QSAR studies using diverse classes of adrenergic antagonists, it appeared of interest to develop a quantitative 3D-QSAR model using the diverse classes of α_{1a}-adrenoreceptor antagonists to find out the essential structural requirements for their antagonistic activity.

Method and Material

The 3D-QSAR studies were performed on 108 chemically diverse molecules belonging to 1,4-benzodioxane, 1,3-dioxolane, spiroethyl-phenylpiperazine, Spiroalkyl 2,5-dichlorophenylpiperazine related compounds, substituted piperazine, Imido derivatives, non-imidospiro derivatives and prazosin related compounds reported in the literature (Quaglia *et al.*,1999; Quaglia *et al.*,2002; Brasili *et al.*, 2003; Rosini *et al.*,2003; Leonardi *et al.*,2004; Quaglia *et al.*, 2005; Quaglia *et al.*, 2008; Franchini *et al.*, 2009; Sorbi *et al.*,2009). The α_1-AR antagonistic activity/ binding affinity data of these compounds are expressed as Ki value in the nanomolar (nM) range. The selected compounds with diverse structural features cover a wide range of biological activity spanning over more than four log units (0.05–2684 nM). A correction factor for 20% lesser value of the activity data has been applied for the compounds reported in the paper (Leonardi *et al.*, 2004) since the reference compound BMY 7378 showed 20% higher activity value than reported in other paper considered in the QSAR study. The Ki values were converted into log Ki (pKi) for use in the QSAR studies.

Rational division of training and test sets

The 108 compounds in the dataset were unbiased distributed into 5 clusters according to their biological activity data and the training set compounds were picked up from generated clusters. It has been suggested that the generated models should be tested on a sufficiently large test set to establish a reliable QSAR model (Prathipati *et al.*, 2003) therefore, the **molecules** were rationally divided into training set of 45 (marked with aestrick,*) and test set of 63 compounds respectively in such a way that they cover almost entire range of biological activity. (Fig.1 and Table. 1-6).

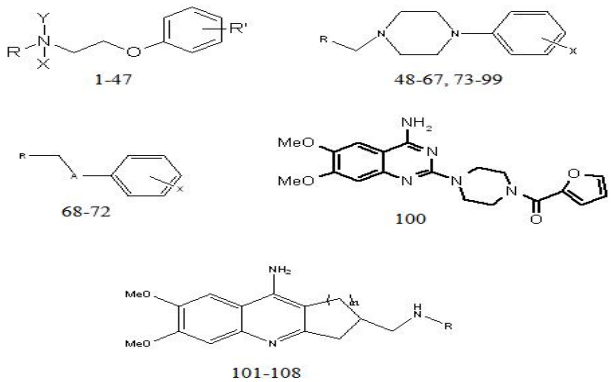

Fig.1 Common Structure of the α_{1a}-AR antagonists used in the 3D-QSAR study

Table. 1. Structure of the molecules (1to 47) used in the 3D QSAR study.

Comp. Name	**R**	**X**	**Y**	**R'**	**Ki (nM)**	**pki**	**Predicted pKi (CoMFA)**	**Predicted pKi (CoMSIA)**
1*	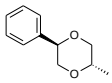	H	-	H	537.03	6.27	6.35	6.583
2	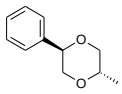	H	-	2-OCH_3	158.49	6.8	6.407	6.624
3	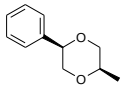	H	-	2-OCH_3	463.52	6.36	6.57	7.288
4*	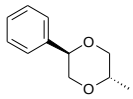	H	-	2,6$(OCH_3)_2$	512.86	6.29	6.616	6.533
5*	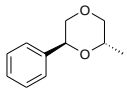	H	-	H	407.38	6.39	6.143	6.194
6	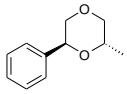	H	-	2-OCH_3	87.09	7.06	6.896	7.137
7	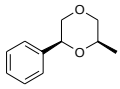	H	-	2-OCH_3	199.53	6.7	6.273	6.083
8*	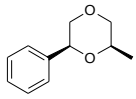	H	-	2,6$(OCH_3)_2$	467.74	6.33	6.653	6.397
9*	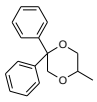	H	-	H	223.87	6.65	6.487	6.588
10*		H	-	2-OCH_3	74.13	7.13	6.926	6.501
11	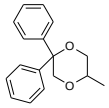	H	-	2,6$(OCH_3)_2$	89.12	7.05	7.342	6.952

12*	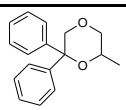	H	-	H	169.82	6.77	6.339	6.418
13	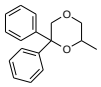	H		2-OCH_3	27.54	7.57	6.857	6.998
14*	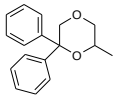	H	-	2,6$(OCH_3)_2$	338.84	6.47	6.651	6.682
15	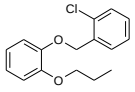	H	-	2,6$(OCH_3)_2$	1.41	8.85	8.546	8.86
16*	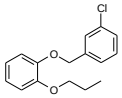	H	-	2,6$(OCH_3)_2$	0.251	9.6	9.142	9.243
17	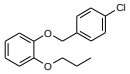	H	-	2,6$(OCH_3)_2$	0.251	9.6	9.139	9.257
18	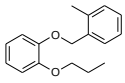	H	-	2,6$(OCH_3)_2$	1.58	8.8	8.624	8.958
19	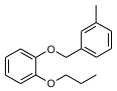	H	-	2,6$(OCH_3)_2$	0.398	9.4	8.96	9.103
20*	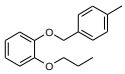	H	-	2,6$(OCH_3)_2$	1.99	8.7	9.033	9.108
21	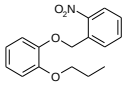	H	-	2,6$(OCH_3)_2$	7.94	8.1	8.976	8.856
22*	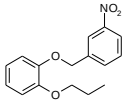	H	-	2,6$(OCH_3)_2$	0.316	9.5	9.37	9.539
23	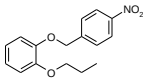	H	-	2,6$(OCH_3)_2$	1.25	8.9	8.76	8.786
24	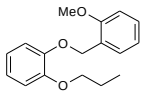	H	-	2,6$(OCH_3)_2$	1.99	8.7	9.02	9.235
25*	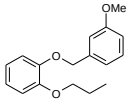	H	-	2,6$(OCH_3)_2$	1.99	8.7	8.523	8.813

26	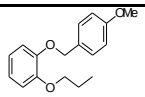	H	-	$2,6(OCH_3)_2$	1.99	8.7	8.728	8.986
27	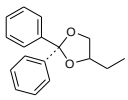	H	H	$2\text{-}OCH_3$	37.15	7.61	6.567	6.846
28	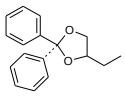	H	H	H	831.76	7.43	6.25	6.698
29*	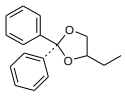	H	CH_3	H	33.88	6.08	6.066	6.314
30*	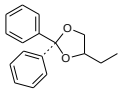	CH_3	CH_3	H	24.54	7.47	7.459	7.326
31*		H	-	$2,6(OCH_3)_2$	0.05	10.3	10.047	9.966
32*	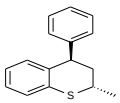	H	-	$2,6(OCH_3)_2$	2.34	8.63	8.921	8.922
33*	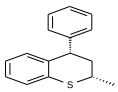	H	-	$2,6(OCH_3)_2$	0.08	10.05	10.138	10.198
34	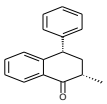	H	-	$2,6(OCH_3)_2$	0.251	9.6	8.694	8.814
35	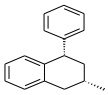	H	-	$2,6(OCH_3)_2$	0.512	9.29	10.22	10.16
36	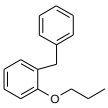	H	-	$2,6(OCH_3)_2$	0.398	9.4	10.06	9.9
37*	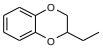	H	-	$2,6(OCH_3)_2$	0.426	9.37	9.232	9.49
38	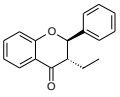	H	-	$2,6(OCH_3)_2$	0.602	9.22	9	9.157

39	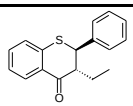	H	-	2,6(OCH_3)$_2$	38.01	7.42	9.049	8.982
40*	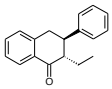	H	-	2,6(OCH_3)$_2$	8.7	8.06	8.176	7.759
41	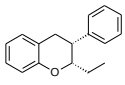	H	-	2,6(OCH_3)$_2$	165.96	6.78	7.985	8.227
42	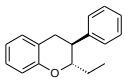	H	-	2,6(OCH_3)$_2$	3.23	8.49	8.911	9.015
43	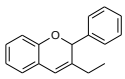	H	-	2,6(OCH_3)$_2$	72.44	7.14	8.751	8.75
44	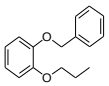	H	-	2,6(OCH_3)$_2$	0.467	9.33	8.754	8.771
45	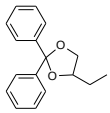	H	-	-	165.95	6.78	7.412	7.294
46	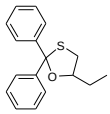	H	-	-	223.82	6.65	7.613	6.965
47		H	-	-	75.85	7.12	7.257	6.914

Table. 2. Structure of the molecules (48to 67) used in the 3D QSAR study.

Comp. Name	**R**	**X**	**Ki (nM)**	**pKi**	**Predicted pKi (CoMFA)**	**Predicted pKi (CoMSIA)**
48.*	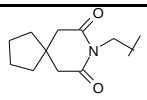	H	2684	5.57	6.123	6.23
49.	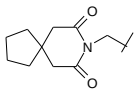	2-Cl	441.288	6.36	6.522	6.416

50.*	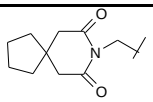	2-$OCH(CH3)_2$	2.832	8.55	8.861	8.56
51.	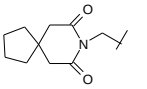	2-CH_3	467.328	6.33	6.564	6.44
52.*	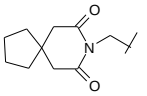	2-CN	170.88	6.77	6.635	6.415
53.	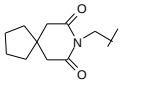	2-Br	301.128	6.52	6.539	6.501
54.	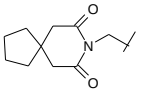	2,5-dichloro	102.4	6.99	6.666	6.733
55.	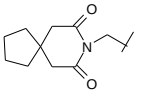	2-cyclopropyl	8.712	8.51	8.626	8.356
56.	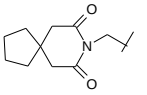	2,5-difluro	108.096	6.97	6.166	6.373
57.*	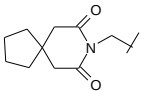	2-Cl, 5-CH_3	100.44	7	6.64	6.456
58.*	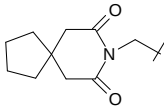	2,5-$(CH_3)_2$	95.424	7.02	7.512	7.473
59.	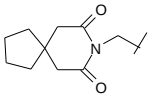	2-Cl, 5-NO_2	35.168	7.45	7.166	7.104
60.	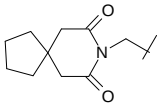	2-CH_3, 5-Cl	152.2	6.82	6.549	6.703
61.	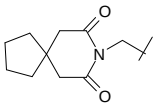	2,5-dibromo	91.248	7.04	6.941	6.784
62.*	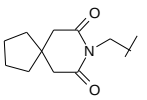	2-CN, 5-Cl	402.56	6.39	6.694	6.528

63.*	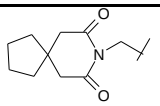	2-Cl, 5-F	86.16	7.06	7.147	7.228
64.	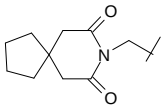	2-Cl, 5-I	383.6	6.42	6.643	6.923
65.	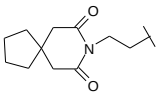	2,5-dichloro	2.28	8.64	8.083	8.51
66.*	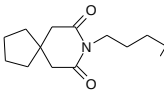	2,5-dichloro	1.448	8.84	9.019	8.793
67.*	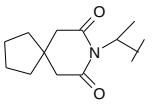	2,5-dichloro	149.344	6.82	6.789	6.887

Table. 3. Structure of the molecules (68 to 72) used in the 3D QSAR study.

Comp. Name	**R**	**A**	**X**	**Ki (nM)**	**pKi**	**Predicted pKi (CoMFA)**	**Predicted pKi (CoMSIA)**
68.	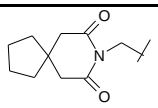	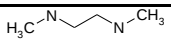	2,5-dichloro	629.04	6.2	5.991	6.381
69.	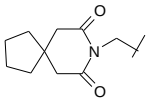	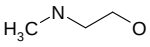	2,5-dichloro	331.28	6.48	6.117	6.3
70.*	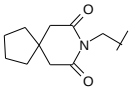	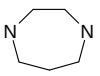	2-Cl	236.08	6.63	6.633	6.461
71.	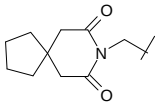	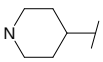	2,5-dichloro	94.992	7.02	7.351	7.176
72.	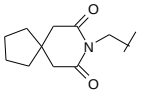	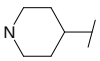	2-Cl	1.608	8.79	8.408	8.213

Table. 4. Structure of the molecules (73 to 99) used in the 3D QSAR study.

Comp. Name	R	X	Ki (nM)	pKi	Predicted pKi (CoMFA)	Predicted pKi (CoMSIA)
73.	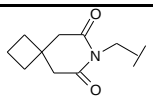	2,5-dichloro	95.68	7.02	6.828	6.977
74.	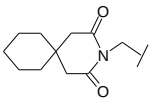	2,5-dichloro	264.408	6.58	6.835	6.866
75.	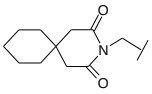	2-Cl	337.28	6.47	6.732	6.628
76.	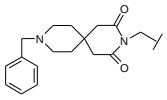	2-OMe	235.52	6.63	7.397	6.974
77.	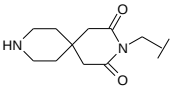	2-OMe	504.672	6.3	6.806	7.039
78.	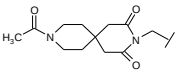	2-OMe	1214.96	5.91	6.674	6.983
79.	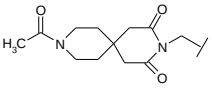	2,5-dichloro	47.856	7.32	6.876	6.312
80.	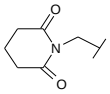	2,5-dichloro	62.304	7.2	6.849	6.183
81.		2,5-dichloro	73.568	7.13	7.172	6.931
82.*	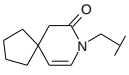	2-Cl	43.144	7.36	7.302	7.276
83.*	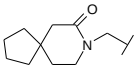	2-Cl	70.04	7.15	7.18	6.897
84.*	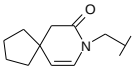	2-OMe	23.4	7.63	7.659	7.896

85.	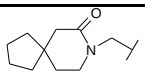	2-OMe	43.544	7.36	7.55	7.575
86.	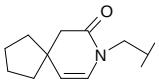	2,5-dichloro	21.768	7.66	7.652	8.14
87.*	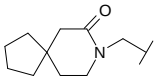	2,5-dichloro	33.928	7.47	7.462	7.348
88.*	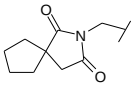	2,5-dichloro	54.608	7.26	7.164	7.207
89.*	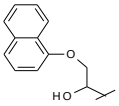	2-OMe	5.88	8.23	8.221	8.33
90.*	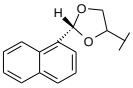	2-OMe	36.3	7.44	7.601	7.506
91.*	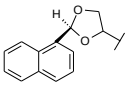	2-OMe	7.94	8.1	7.817	7.576
92.	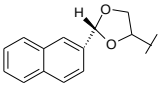	2-OMe	15.13	7.82	8.007	7.282
93.	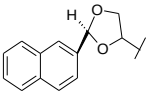	2-OMe	34.67	7.46	7.328	7.379
94.*	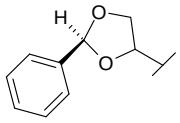	2-OMe	28.84	7.54	7.538	7.263
95.	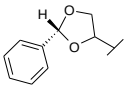	2-OMe	2.69	8.57	7.409	7.515
96.	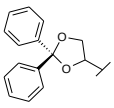	2-OMe	0.26	9.58	7.635	7.947
97.*	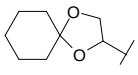	2-OMe	91.2	7.04	7.164	6.98

98.	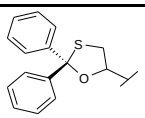	2-OMe	2.04	8.69	6.73	7.139
99.	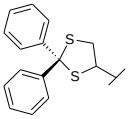	2-OMe	57.5	7.24	7.461	7.717

Table. 5. Structure of the molecules (100) used in the 3D QSAR study.

Comp. Name	**Structure**	**Ki (nM)**	**pKi**	**Predicted pKi (CoMFA)**	**Predicted pKi (CoMSIA)**
100*	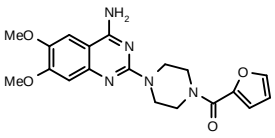	0.588	9.23	8.972	9.215

Table. 6. Structure of the molecules (101to 108) used in the 3D QSAR study.

Comp. Name	**R**	**n**	**Ki (nM)**	**pKi**	**Predicted pKi (CoMFA)**	**Predicted pKi (CoMSIA)**
101*	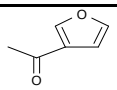	2	95.49	7.02	6.811	6.925
102*	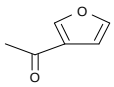	1	158.49	6.8	6.849	6.884
103	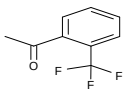	2	288.4	6.54	6.217	6.219
104	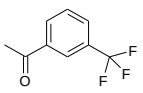	2	31.62	7.5	7.155	7.385

105*	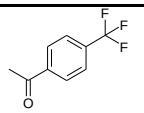	2	85.11	7.07	6.937	6.976
106	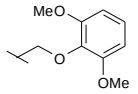	2	977.24	6.01	6.136	6.374
107*		2	2570.4	5.59	5.469	5.936
108*	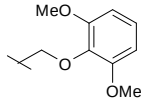	2	1698.2	5.77	5.502	5.969

Computational approach and Molecular alignment

Molecular modeling studies *viz.* CoMFA and CoMSIA were done on a Silicon Graphics Octane R12000 workstation using SYBYL6.9 molecular modeling software (Tripos, St.Louis, MO). All compounds were built using the most active compound **31** as a template in the ISIS Draw 2.5 and thereafter imported in sybyl 6.9.The partial charges for all compounds were calculated using Gasteiger–Huckel method and optimized for their geometry using Tripos force field with a distance dependent dielectric function and energy convergence criterion of 0.001 kcal/mol Å using 1000 iterations and standard SYBYL settings. Alignment is a critical step in the CoMFA studies and among the various approaches, the three more commonly suggested alignments in the literature are maximum common structure (MCS) based alignment, rigid body field fit alignment and multifit alignment (Kuldeep *et al.*, 2008).

In the present study the MCS based alignment was used as it has given the best result in present case and the core (Bold Structure) of the most active compound **31** (Fig. 2) has been used for common structure based alignment (Fig. 3).

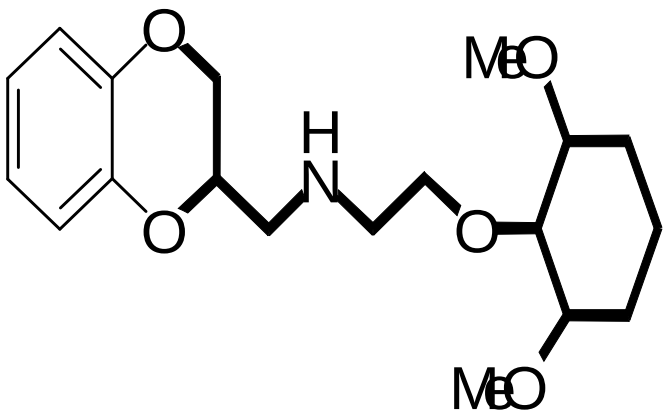

Fig. 2. The core of the most active compound 31 used for the alignment

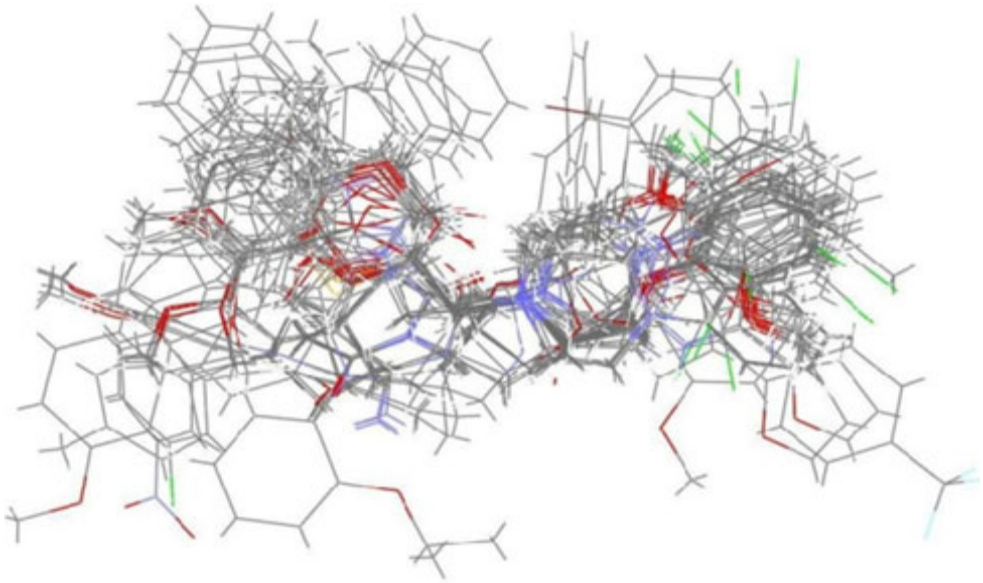

Fig. 3. The overall alignment of the molecules used in the 3D-QSAR study.

CoMFA Studies

The steric(Lennard–Jonnes potentials) and electrostatic fields(Coulombic potentials) for CoMFA were calculated for aligned molecules which were kept in 3D cubic lattice with a grid spacing of 2.0 Å in x, y and z directions using Tripos module in SYBYL. For each alignment a sp^3 carbon atom having a charge of +1 and a radius of 1.52 Å was used as a probe to calculate various steric and electrostatic fields. The influence of different parameter settings on CoMFA, various steric and electrostatic cutoffs and grid spacing were also tried as suggested by Crammer *et al.* (Crammer *et al.*, 1988).

CoMSIA studies

The CoMSIA technique is based on the molecular similarity indices with the same lattice box used for the CoMFA calculations (Klebe *et al.* 1994). It is considered superior than the CoMFA technique in certain aspects like remains unaffected to both, region shifts as well as small shifts within the alignments; no need of steric cutoffs and more intuitively interpretable contour maps. In the present study, standard settings of CoMSIA (Probe with charge +1, radius 1 Å and hydrophobicity +1, hydrogen-bond donating +1, hydrogen-bond accepting +1, attenuation factor of 0.3 and grid spacing 2 Å) were used to calculate five different fields *viz* steric, electrostatic, hydrophobic, acceptor and donor.

Partial least square analysis

PLS is used to correlate α_{1a}-adrenoreceptor antagonistic activity with the CoMFA and CoMSIA values containing magnitude of steric, electrostatic and hydrophobic potentials. The leave one out (LOO) cross-validation procedure by SAMPLS method was used to assess the models as implied in SYBYL (Bush *et al.*, 1993). In addition to LOO cross validation a group cross validation using 30 groups, repeating the procedure 30 times was also carried out. The mean of

30 readings is given as $r^2_{cv(mean)}$. The full PLS analysis was carried out with a column filtering of 2.0 kcal/mol to speed up the calculation and reduce the noise.

Results and discussion

The CoMFA and CoMSIA are highly sensitive to the relative alignment of molecules and since these molecules have widely varying structures, it was important to determine the best alignment rule. The MCS based alignment method was found to be best as it exhibited high q^2 values both for CoMFA (q^2 = 0.709) as well as CoMSIA (q2 = 0.648). Since the MCS based alignment method gave the model with best statistics and reasonable superimposition of important functional groups (Fig. 2), this alignment was further used for systematic CoMFA and CoMSIA studies using the training set compounds (total 45). The results have been summarized in Tables 7.

Table 7. PLS statistics of CoMFA (TS) and CoMSIA (SEH) models

Parameters		**CoMFA (TS)**	**CoMSIA (SEH)**
q^2		**0.709**	**0.648**
PRESS		**0.687**	**0.756**
r^2		**0.962**	**0.949**
SEE		**0.247**	**0.287**
F		**199.628**	**146.269**
N		**5**	**5**
	S	**0.515**	**0.211**
Fractions	**E**	**0.485**	**0.459**
	H	**-**	**0.330**
r^2_{bs} (30runs)		**0.979**	**0.966**
SD_{bs}		**0.009**	**0.009**
$r^2_{CV\ (mean)}$ (30runs)		**0.714**	**0.649**
r^2_{pred}		**0.629**	**0.656**

q^2 = leave one out cross-validation correlation coefficient; PRESS = LOO cross-validated standard error; r^2 = conventional correlation; SEE = standard error of estimate; F = degree of freedom; N = optimal number of component; r^2_{bs} = bootstrapping correlation; SD_{bs} = bootstrapping standard deviation; $r^2_{CV(mean)}$ = group cross-validation; TS = Tripos standard; SEA = Steric, electrostatic and Acceptor

CoMFA analysis

In CoMFA and CoMSIA studies a q^2 value of 0.3 is considered statistically significant (Bohm *et al.*, 1919) while a q^2 value of 0.4 is generally considered better. Therefore the CoMFA models having $q^2 > 0.5$ can be considered more significant statistically. The Tripos standard (TS) field showed the highest q^2 of 0.709 using 5 principal components with a high conventional r^2 value of 0.962 and low standard error of estimate (0.247) indicates a statistically highly significant model. To further assess the robustness of the models, bootstrapping analysis (30 runs) was performed and r^2 bs of 0.979 (SD_{bs} = 0.009) was obtained, further establishing the strength of the model. In addition to LOO, a group cross-validation was further done to assess the internal predictive ability of the model, cross-validation for 30 times was performed with 30 groups and the mean r^2_{CV} of 0.714 (TS) reveals that the models have good internal predictivity and the results were not based on chance correlation (Table 3). A test set of 63 molecules were used to evaluate the predictability of the generated model and a predictive r^2 of 0.629 showed the predictive ability of the generated model (Fig. 4A). The Predictive pKi value of the training set as well as test set molecules based on the CoMFA model has been included in the Tables 1-6.

CoMSIA analysis

Various CoMSIA models were generated considering all possible combinations of field descriptors. In this study, steric(S), electrostatic (E) and hydrophobe (H) field descriptors were found to have important role in modulation of biological activity. Several of the models were found to have high statistical significance. The model having steric and electrostatic and acceptor fields gave the highest q^2 of 0.648 at 5 components among generated CoMSIA models and a conventional noncross-validated r^2 of 0.949 (Table 4). To further assess the statistical ability and the robustness of the model, bootstrapping analysis (30 runs) was performed and r^2_{bs} of 0.966 with low standard deviation of 0.012 was obtained showing robustness of the models. Similar to CoMFA, to assess the internal predictive ability of the model, group cross-validation was performed with 30 groups and the mean r^2_{cv} of 0.649 reveals that these models have high internal predictivity. A predictive r^2 of 0.656 for the 63 test set compounds showed the usefulness of the model (Fig.4B). The Predictive pKi value of the training set as well as test set molecules based on the CoMSIA model has been included in the Tables 1-6..

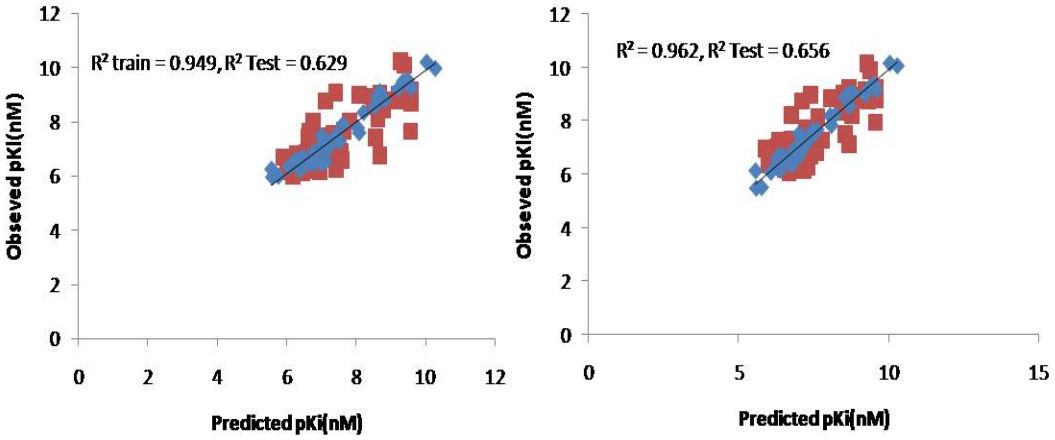

Figure 4. Correlation graph between observed and predicted activities of training set (Blue) and test set (Red) molecules ; (A) CoMFA and (B) CoMSIA.

CoMFA and CoMSIA contour maps

The analysis of the CoMFA and CoMSIA contour maps provides good insight into the SAR by providing a visual display of favored and disfavored positions. Therefore, the steric and electrostatic features of the final CoMFA and CoMSIA models are displayed as contour maps of the PLS regression coefficients at each CoMFA/ CoMSIA region grid point. They are generated using the field type StDev*Coefficient to show the contribution for favourable and unfavorable interactions with the receptor in terms of steric (80% green, 20% yellow), electrostatic (80% blue and 20% red), hydrophobic (80% yellow, 20% white), donor (80% cyan, 20% purple) and acceptor (80% magenta, 20% red). These contour maps for the 3D models are shown in Fig. 5.

The surfaces near the template molecule **31** indicate the regions where the increase (green region) or decrease (yellow region) in steric bulk as well as increase (blue region) or decrease (red region) in electrostatic field would be important for the improvement of binding affinity. The yellow polyhydra in the hydrophobic contours shows the region where an increase in hydrophobicity is favourable for α_{1a}-adrenoreceptor antagonistic activity while white polyhydra denotes the region where hydrophobicity is unfavorable for activity. The advantage of CoMSIA contour maps over CoMFA is that they are easier to interpret.

The CoMFA contours mainly showed four types of regions (Fig.5A). The first region is where the green polyhedra is largest (near the phenylchroman group) and signifies the importance of bulky steric group at this region which may be important for hydrophobic interaction with the receptor. The second one is blue polyhedra near the chroman moiety and phenoxy oxygen atom of the molecule **31** showed that there could be possibility of H- bond interaction at the binding site involving the oxygen atom of this molecule. The third yellow and fourth red polyhedral regions described the undesired steric group. Fourth red polyhedral region showed that the addition of negatively charged group at this region may increase in adrenergic antagonistic activity. The steric and electrostatic CoMSIA contours are also in well agreement with the CoMFA contours as shown in Fig.5B.The contour plot of hydrophobic field as shown by white polyhydra (Fig. 5C) also suggested the importance of hydrophobic interaction near the phenylchroman group of the most active molecule **31** of the dataset.

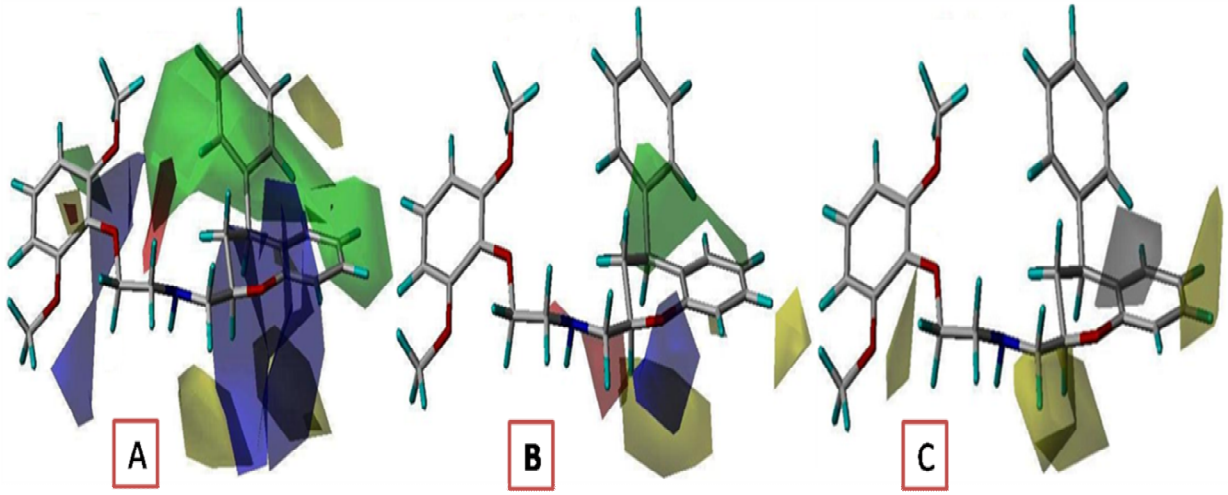

Figure 5:(A) The steric (Green and Yellow), electrostatic (Blue and Red) contours of CoMFA (B) The steric (Green and Yellow), electrostatic (Blue and Red) contours of CoMSIA and (C) hydrophobic (white and yellow) contours of CoMSIA displayed around the most active compound **31**.

Conclusion

The CoMFA and CoMSIA method has been applied successfully to rationalize the structurally diverse α_{1a}-ARs antagonists covering a wide range of biological activity and structural features in terms of their steric, electrostatic and hydrophobic properties. The developed models showed good statistical significance in internal (q^2, group cross-validation and bootstrapping) validation and performed very well in predicting the biological activity (pKi) of the compounds in the test set. In view of the above, it may be concluded that the developed CoMFA and CoMSIA model can further be applied for the identification and optimization of novel scaffolds with potent α_{1a}–adrenergic receptor antagonistic activity.

Acknowledgement

The technical assistance of Mr. A.S. Kushwaha is gratefully acknowledged during this work. One of the authors AKG acknowledges CSIR, New Delhi for financial support.**CDRI Communication No. 7942.**

References

Barbaro R., Betti L., Botta M., Corelli F., Giannaccini G., Maccari L., Manetti F., Strappaghetti G., Corsano S. (2001) Synthesis, biological evaluation, and pharmacophore generation of new pyridazinone derivatives with affinity toward α1- and α2-adrenoceptors. J. Med. Chem. 44:2118–2132.

Bohm M., Sturzebecher J., Klebe G. (1999) Three-dimensional quantitative structure-activity relationship analysis using comparative molecular field analysis and comparative molecular similarity indices analysis to elucidate selectivity differences of inhibitors binding to trypsin, thrombin, and factor Xa. J. Med. Chem. 42:458–477.

Brasili L., Sorbi C., Franchini S., Manicardi M., Angeli P., Marucci G., Leonardi A., Poggesi E. (2003) 1,3-Dioxolane-Based Ligands as a Novel Class of 1-Adrenoceptor Antagonists. J. Med. Chem. 46: 1504-1511.

Bush B. L., Nachbar R. B. (1993) Sample-distance partial least squares: PLS optimized for many variables, with application to CoMFA. J. Comput. Aided Mol. Des. 7: 587–619.

Cramer III R. D., Patterson D. E., Bunce J. D. (1988) Comparative molecular field analysis (CoMFA): Effect of shape on binding of steroids to carrier proteins. J. Am. Chem. Soc.110:5959–5967.

Debnath B., Samanta S., Naskar S. K., Roy K., Jha T. (2003) QSAR Study on the Affinity of Some Arylpiperazines towards the 5-HT1A/α1-Adrenergic Receptor Using the E-State Index. Bioorg. Med. Chem. Lett. 13: 2837-2842.

Evers A. Klabunde T. (2005) Structure-based Drug Discovery Using GPCR Homology Modeling: Successful Virtual Screening for Antagonists of the Alpha1A Adrenergic Receptor. J. Med. Chem. 48: 1088–1097.

Fang H., Lu J.-F., Xia L. (2003) Constructing biophore of uroselective a1-adrenoceptor antagonist. J. Chin. Pharm. Sci. 12:188–191.

Franchini S., Tait A., Prandi A., Sorbi C., Gallesi R., Buccioni M., Marucci G., DeStefani C., Cilia A., Brasili L. (2009) (2,2-Diphenyl-[1,3]oxathiolan-5-ylmethyl)-(3-phenylpropyl)-amine: a Potent and Selective 5-HT1A Receptor Agonist. ChemMedChem. 4: 196 – 203.

Fumagalli L., Bolchi C., Colleoni S., Gobbi M., Moroni B., Pallavicini M., Pedretti A., Villa L., Vistoli G., Valoti E. (2005) QSAR study for a novel series of ortho monosubstituted phenoxy analogues of α1-adrenoceptor antagonist WB4101. Bioorg. Med. Chem. 13: 2547-2559.

Jain K.S., Bariwal J.B., Kathiravan M. K., Phoujdar M. S., Sahne R. S., Chauhan B. S., Shah A. K., Yadav M. R. (2008) Recent advances in selective α1-adrenoreceptor antagonists as antihypertensive Agents. Bioorg. Med. Chem. 16: 4759-4800.

Klabunde T., Evers A. (2005) GPCR antitarget modeling: pharmacophore models for biogenic amine binding GPCRs to avoid GPCR-mediated side effects. ChemBioChem. 6: 876–889.

Klebe G., Abraham U., Mietzner T. (1994) Molecular Similarity Indices in a Comparative Analysis (CoMSIA) of Drug Molecules to Correlate and Predict Their Biological Activity. J. Med. Chem., 37: 4130–4146.

Kuldeep K.K., Dixit A., Saxena A.K.(2008) An investigation of structurally diverse carbamates for acetylcholinesterase (AChE) inhibition using 3D-QSAR analysis. J. Mol. Graph. Model. 27: 197-208.

Kulig K., Sapa J., Nowaczyk A., Filipek B., Malawska B. (2009) Design, synthesis and pharmacological evaluation of new 1-[3-(4-arylpiperazin-1-yl)-2-hydroxy-propyl]-3,3-diphenylpyrrolidin-2-one derivatives with antiarrhythmic, antihypertensive, and a-adrenolytic activity. Eur. J. Med. Chem. 44:3994-4003.

Leonardi A, Barlocco D., Montesano F., Cignarella G., Motta G., Testa R., Poggesi E., Seeber M., De Benedetti P.G., Fanelli F. (2004) Synthesis, screening, and molecular modeling of new potent and selective antagonists at the α_{1d} -adrenergic receptor. J. Med. Chem. 47: 1900-1918.

Li M.Y., Tsai K.-C., Xia L. (2005) Pharmacophore identification of α_{1a}-adrenoceptor antagonists. Bioorg. Med. Chem. Lett. 15:657–664.

Li M.Y., Xia L. (2007) Rational design, synthesis, biological evaluation, and structure–activity relationship studies of novel 1-Indanone α_1-adrenoceptor antagonists. Chem. Biol. Drug Des. 70: 461 – 464.

MacDougall I.J.A., Griffith R. (2006) Selective pharmacophore design for α1-adrenoceptor subtypes. J. Mol. Graph. Model. 25: 146-157.

Maciejewska D., ołek T. Z, Herold F. (2006) CoMFA methodology in structure-activity analysis of hexahydro- and octahydropyrido[1,2-c]pyrimidine derivatives based on affinitytowards 5-HT1A, 5-HT2A and α1-adrenergic receptors. J. Mol. Graph. Model. 25:353–362.

Nowaczyk A., Kulig K., Malawska B. (2009) 1-(3-(4-Arylpiperazin-1-yl)-propyl)-Pyrrolidin-2-one derivatives as α_1-adrenoceptor antagonists: A QSAR study. QSAR Comb. Sci. 28: 979-988.

Pallavicini M., Fumagalli L., Gobbi M., Bolchi C., Colleoni S., Moroni B., Pedretti A., Rusconi C., Vistoli G., Valoti E. (2006) QSAR study for a novel series of ortho disubstituted phenoxy analogues of α1-adrenoceptor antagonist WB4101. Eur. J. Med. Chem. 41:1025-1040.

Pedretti A., Silva M.E., Villa L. Vistoli G. (2004) Binding site analysis of full-length α1a adrenergic receptor using homology modeling and molecular docking. Biochem. Biophys. Res. Commun. 319: 493-500.

Prathipati P., Saxena A.K. (2003) Comparison of MLR. PLS and GA-MLR in QSAR analysis. SAR QSAR Environ. Res. 14: 433–446.

Quaglia W., Piergentili A., Bello F.D., Farande Y., Giannella M., Pigini M., Rafaiani G., Carrieri A., Amantini C., Lucciarini R., Santoni G., Poggesi E., Leonardi A. (2008) Structure activity relationships in 1,4-Benzodioxan-Related Compounds. 9.(1) From 1,4-Benzodioxane to 1,4-

dioxane ring as a promising template of novel α_{1D}-adrenoreceptor antagonists, 5-HT_{1A} full agonists, and cytotoxic agents. J. Med. Chem. 51: 6359-6370.

Quaglia W., Pigini M., Piergentili A., Giannella M., Gentili F., Marucci G., Carrieri A., Carotti A., Poggesi E., Leonardi A., Melchiorre C. (2002) Structure−Activity Relationships in 1,4-benzodioxan-related compounds. 7. selectivity of 4-phenylchroman analogues for α_1−adrenoreceptor subtypes. J. Med. Chem. 45: 1633-1643.

Quaglia W., Pigini M., Piergentili A., Giannella M., Marucci G., Poggesi E., Leonardi A., Melchiorre C. (1999) Structure−activity relationships in 1,4-benzodioxan-related compounds. 6. role of the dioxane unit on selectivity for 1-adrenoreceptor subtypes. J. Med. Chem. 42 : 2961-2968.

Quaglia W., Santoni G., Pigini M., Piergentili A., Gentili F., Buccioni M., Mosca M., Lucciarini R., Amantini C., Nabissi M.I., Ballarin P. I., Poggesi E., Leonardi A., Giannella M. (2005) Structure−activity relationships in 1,4-benzodioxan-related compounds.8.[1]{2-[2-(4-chlorobenzyloxy)phenoxy]ethyl}-[2-(2,6-dimethoxyphenoxy)ethyl]amine clopenphendioxan) as a tool to highlight the involvement of 1d- and 1β-adrenoreceptor subtypes in the regulation of human pc-3 prostate cancer cell apoptosis and proliferation. J. Med. Chem. 48: 7750-7763.

Romeo G., Materia L., Manetti F., Cagnotto A., Mennini T., Nicoletti F., Botta M., Russo F., Minneman K.P. (2003) New pyrimido[5,4-b]indoles as ligands for a1-adrenoceptor subtypes. J. Med. Chem. 46 2877–2894.

Rosini M., Antonello A., Cavalli A., Bolognesi M.L., Minarini A., Marucci G., Poggesi E., Leonardi A., Melchiorre C. (2003) Prazosin-related compounds: effect of transforming the piperazinylquinazoline moiety into an aminomethyltetrahydroacridine system on the affinity for 1-adrenoreceptors. J. Med. Chem. 46: 4895-4903.

Shakya N., Fatima Z., Saxena A.K. (2004) 3D-QSAR studies on substituted dihydropyridines for their α_{1a}-adrenergic receptor binding affinity. Med. Chem. Res. 13:812-823.

Sorbi C., Franchini S., Tait A., Prandi A., Gallesi R., Angeli P., Marucci G., Pirona L., Poggesi E., Brasili L. (2009) 1,3-Dioxolane-based ligands as rigid analogues of naftopidil: structure–affinity/activity relationships at a1 and 5-ht1a receptors. ChemMedChem, 4:393-399.

Tripos Inc., 1699, South Hanley Road, St. Louis, MO 63144.